This article was downloaded by: [Institute Of Atmospheric Physics]
On: 09 December 2014, At: 15:15
Publisher: Taylor & Francis
Informa Ltd Registered in England and Wales Registered Number: 1072954 Registered office: Mortimer House, 37-41 Mortimer Street, London W1T 3JH, UK

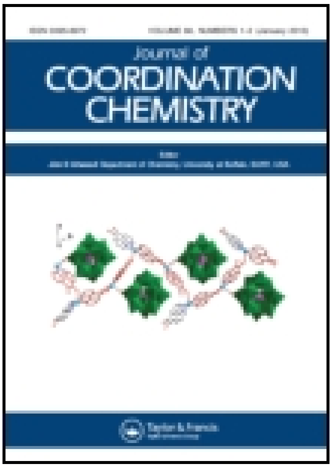

Click for updates

Journal of Coordination Chemistry
Publication details, including instructions for authors and subscription information:
http://www.tandfonline.com/loi/gcoo20

Structure and magnetism of a new 2-D trinuclear Mn(II) polymer

Lu Lu[ab], Fu-Min Wang[c], Jun Wang[ab], Bin Xie[ab] & Jian-Qiang Liu[d]
[a] Institute of Functionalized Materials, Sichuan University of Science & Engineering, Zigong, PR China
[b] School of Chemistry and Pharmaceutical Engineering, Sichuan University of Science & Engineering, Zigong, PR China
[c] Department of Chemistry and Chemical Engineering, Shaanxi Xueqian Normal University, Xian, PR China
[d] School of Pharmacy, Guangdong Medical College, Dongguan, PR China

Accepted author version posted online: 07 Jul 2014.Published online: 12 Aug 2014.

To cite this article: Lu Lu, Fu-Min Wang, Jun Wang, Bin Xie & Jian-Qiang Liu (2014) Structure and magnetism of a new 2-D trinuclear Mn(II) polymer, Journal of Coordination Chemistry, 67:13, 2271-2279, DOI: 10.1080/00958972.2014.941829

To link to this article: http://dx.doi.org/10.1080/00958972.2014.941829

PLEASE SCROLL DOWN FOR ARTICLE

Taylor & Francis makes every effort to ensure the accuracy of all the information (the “Content”) contained in the publications on our platform. However, Taylor & Francis, our agents, and our licensors make no representations or warranties whatsoever as to the accuracy, completeness, or suitability for any purpose of the Content. Any opinions and views expressed in this publication are the opinions and views of the authors, and are not the views of or endorsed by Taylor & Francis. The accuracy of the Content should not be relied upon and should be independently verified with primary sources of information. Taylor and Francis shall not be liable for any losses, actions, claims, proceedings, demands, costs, expenses, damages, and other liabilities whatsoever or howsoever caused arising directly or indirectly in connection with, in relation to or arising out of the use of the Content.

This article may be used for research, teaching, and private study purposes. Any substantial or systematic reproduction, redistribution, reselling, loan, sub-licensing, systematic supply, or distribution in any form to anyone is expressly forbidden. Terms &

Journal of Coordination Chemistry, 2014
Vol. 67, No. 13, 2271–2279, http://dx.doi.org/10.1080/00958972.2014.941829

Structure and magnetism of a new 2-D trinuclear Mn(II) polymer

LU LU*†‡, FU-MIN WANG§, JUN WANG†‡, BIN XIE†‡ and JIAN-QIANG LIU¶

†Institute of Functionalized Materials, Sichuan University of Science & Engineering, Zigong, PR China
‡School of Chemistry and Pharmaceutical Engineering, Sichuan University of Science & Engineering, Zigong, PR China
§Department of Chemistry and Chemical Engineering, Shaanxi Xueqian Normal University, Xian, PR China
¶School of Pharmacy, Guangdong Medical College, Dongguan, PR China

(*Received 25 March 2014; accepted 4 June 2014*)

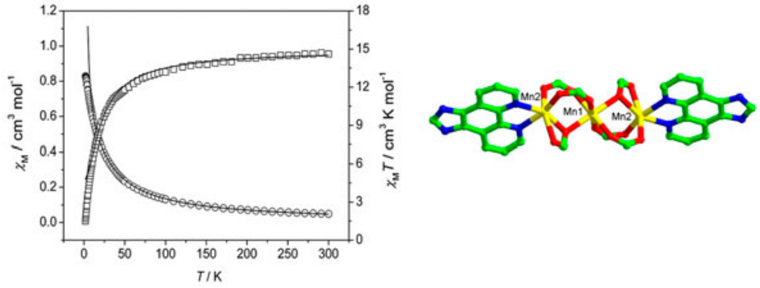

A new complex has been synthesized and structurally characterized. The title compound shows 3D porous network via the packing interactions. In addition, the magnetic property was discussed in compounds **1** in detail.

A new complex, $\{[Mn_3(oba)_2(IP)_2(CH_3COO)_2]\cdot H_2O\}_n$ (**1**) (H_2oba = 4,4′-oxybis(benzoic acid), IP = 1-*H*-imidazo[4,5-f][1,10]-phenanthroline), has been synthesized and structurally characterized by single-crystal diffraction analysis. The structural determination revealed that **1** has a 2-D grid motif, which can be further linked into a 3-D porous network via packing interactions. The magnetic properties of **1** are discussed.

Keywords: Carboxylic acid; Layer; Magnetism

Introduction

Crystal engineering has provided a sound junction between esthetics of architectures and their potential functions [1–4]. Ingenious designs of ligands and proper choice of metal ions

---

*Corresponding author. Email: luluszg@126.com

are keys to achieve the resulting coordination polymers [5]. Flexible di- and poly-carboxylic acids are good candidates for construction of new coordination polymers as the carboxyl groups can form C–O–M–O cyclic mode with metal ions, improving the stability of transition metal complexes. Furthermore, such carboxylic acids have two or more carboxyl groups that can be completely/partially deprotonated, which results in many interesting structures with higher dimensions. 4,4′-Oxybis(benzoic acid) (H_2oba) is a long, V-shaped, flexible ligand; its coordination chemistry has been studied and several coordination polymers have been obtained [6–8]. The magnetic strength and nature of the magnetic coupling between metal centers can be determined by the bridging linkers. Carboxylate linkers have been widely employed to shape molecular magnetic materials owing to their various binding modes that afford superexchange pathways. Design and synthesis of polynuclear metal–carboxylate complexes with predictable magnetic properties are still a challenge in molecular magnetism [9–11].

A mixed-ligand strategy is a good choice for the construction of coordination polymers. Chelating bipyridine-like ligands, such as 1,10-phenanthroline (phen) and 2,2′-bipyridine, are important in maintaining the 1-D of coordination polymers and may provide potential supramolecular recognition sites [12, 13]. Du *et al.* presented the key advances in the design of coordination polymers using mixed-ligand synthetic strategy and discussed the relationship between selected mixed organic ligands and the resulting MOFs [12(b)–(c)]. Herein, we report the synthesis and structure of a new coordination polymer, $\{[Mn_3(oba)_2(IP)_2(CH_3COO)_2]\cdot H_2O\}_n$ (**1**). The magnetic behavior of **1** was also explored.

Experimental

Materials and methods

All reagents were purchased from commercial sources and used as received. IR spectra were recorded with a Perkin-Elmer Spectrum One spectrometer from 4000 to 400 cm^{-1} using KBr pellets. Thermogravimetric analysis (TGA) was carried out with a Mettler-Toledo TA 50 in dry dinitrogen (60 $mL\ min^{-1}$) at a heating rate of 5 $°C\ min^{-1}$. X-ray powder diffraction (XRPD) data were recorded on a Rigaku RU200 diffractometer at 60 kV, 300 mA for Cu K_α radiation ($\lambda = 1.5406$ Å) with a scan speed of 2 $°C\ min^{-1}$ and a step size of 0.013° in 2θ. Magnetic susceptibility data of powdered sample restrained in parafilm were measured on an Oxford Maglab 2000 magnetic measurement system in the temperature range 300–1.8 K and at a field of 1 KOe.

X-ray crystallography

Single-crystal X-ray diffraction analysis of **1** was carried out on a *Bruker SMART APEX II CCD* diffractometer equipped with graphite monochromated Mo Kα radiation ($\lambda = 0.71073$ Å) using ϕ/ω scan technique at room temperature. Data were processed using the Bruker SAINT package and the structure solution and refinement procedure were performed using SHELX-97 [14]. The structure was solved by direct methods and refined by full-matrix least-squares fitting on F^2. The hydrogens of organic ligands were placed in calculated positions and refined riding on attached atoms with isotropic thermal parameters 1.2 times those of their carrier atoms. The hydrogens of lattice waters in **1** were not located using the different Fourier method. The void volume is actually not that large (four times 132 Å^3, which is four times 2% of the unit cell volume). A water molecule would need about 40 cubic Angstroms (see http://www.cryst.chem.uu.nl/spek/platon/pl000302.html). The volume could thus have held three to four H_2O molecules. Squeeze does however show that the voids are mostly empty. Each void of 132 cubic Angstroms holds about seven electrons, thus less than one H_2O, not three to four. The water molecule O8 in **1** has refined better with only two positions slightly off the twofold axis. Table 1 shows crystallographic data of **1**. Selected bond distances and bond angles are listed in table 2. CCDC: 933984.

Synthesis of $\{[Mn_3(oba)_2(IP)_2(CH_3COO)_2]\cdot H_2O\}_n$ *(1)*

A mixture of $MnSO_4\cdot H_2O$ (0.0346 g), H_2oba (0.0516 g), IP (0.0202 g), NaOAc (0.0178 g), CH_3CN (5 mL), and deionized water (5 mL) was stirred for 30 min in air. The pH of the resulting solution was adjusted to 7 using dilute NaOH (1 M L^{-1}) and kept at 160 °C (oven) for 72 h, and then cooled to 25 °C. The resulting crystals were filtered off, washed with water, and dried in air. $C_{58}H_{40}Mn_3N_8O_{15}$ (1253.80). Calcd: C, 55.56; H, 3.21; N, 8.94. Found: C, 54.55; H, 3.17; N, 8.41. IR (KBr, cm^{-1}): 3468(vs), 3098(s), 1605(vs), 1580(m), 1480(s), 1399(vs), 1355(m), 1150(s), 827(s), 647(s).

Table 1. Crystallographic data and structure refinement details for **1**.

Empirical formula	$C_{58}H_{40}Mn_3N_8O_{15}$
Formula mass	1253.80
Crystal system	Monoclinic
Space group	*C2/c*
a (Å)	15.456(10)
b (Å)	14.414(10)
c (Å)	26.684(17)
α (°)	90
β (°)	104.126(12)
γ (°)	90
V (Å^3)	5765(7)
Z	4
D_{Calcd} (g cm^{-3})	1.445
μ (mm^{-1})	0.721
F(0 0 0)	2556
Reflections collected	18,714
R_{int}	0.0432
R_1, wR_2 [$I > 2\sigma(I)$]	0.0425, 0.0921
R_1, wR_2 (all data)	0.0714, 0.1001

Table 2. Selected bond distances (Å) and angles (°) for **1**.

Mn1–O2#1	2.1241(19)	Mn1–O7#1	2.1772(19)
Mn1–O4#2	2.1981(18)	Mn2–O1	2.102(2)
Mn2–O6	2.167(2)	Mn2–O4	2.2450(19)
Mn2–O5	2.329(2)	Mn2–N2	2.303(2)
Mn2–N1	2.251(2)	O2–Mn1–O2	180
O2–Mn1–O7	94.24(8)	O7–Mn1–O7	180
O4–Mn1–O4	180	O4–Mn1–O7	88.90(7)
O4–Mn2–N1	155.26(7)	O1–Mn2–N2	161.20(7)
O5–Mn2–O6	155.03(6)	O1–Mn2–O5	96.44(9)

Note: Symmetric codes: #1: $-x + 3/2$, $-y + 1/2$, $-z + 1$; #2: $-x + 3/2$, $y - 1/2$, $-z + 3/2$.

Results and discussion

$\{[Mn_3(oba)_2(IP)_2(CH_3COO)_2]\cdot H_2O\}_n$ (1)

The structure contains three Mn(II) ions, two IP ligands, two oba ligands, two coordinated acetates, and one lattice water (figure 1). The oba adopts $(k^1–k^1)–(k^1–k^1)–\mu_4$ mode. Mn(1) is located at the inversion site and is coordinated by six *trans*-related carboxylate oxygens from two different oba anions and two acetates in an octahedral geometry. The Mn(2) is six-coordinate in a distorted geometry by four oxygens from three different carboxylic ligands and two nitrogens from one IP molecule. The Mn–O/N bond lengths are within the normal range [15]. The polyhedra of three metals are bridged by carboxylate groups and give centrosymmetric trinuclear manganese(II) subunits (Mn^{II}_3). The Mn(II)···Mn(II) distance within the trinuclear metal unit is 3.51 Å, slightly smaller than those in other carboxylate-bridged trinuclear Mn(II) complexes [16–20]. The shortest distance of inter-Mn^{II}_3 units is 7.02 Å.

Based on these connections, trinuclear manganese(II) subunits (Mn^{II}_3) are bridged by two carboxylates, thus, 2-D layers are formed along the *bc* plane, as shown in figure 2. Interplanar distances between two neighboring aromatic rings of IP and between pyridyl ring (C1, C2, C3, C4, C5, and N1) and imidazole ring (C11, C12, C13, N3, and N4) are ca. 3.88(2) Å, indicating the presence of face-to-face π–π stacking interaction. There is also a π–π stacking interaction of 3.90(5) Å between pyridyl ring (C1, C2, C3, C4, C5, and N1) and pyridyl ring (C1A, C2A, C3A, C4A, C5A, and N1A). A 3-D supramolecular motif is formed via the weak interaction (figure 3) [21].

Lei and co-workers reported $[Mn_3(oba)_3(2,2'\text{-bipy})_2]_n$, which shows a 3-D unusual (2,6)-connectivity $(8^{12}.12^3)(8)(3)$ topology. The manganese trimetallic unit bridged by six carboxylic groups constitutes a trimetallic second building unit $[Mn_3(CO_2)_6]$ [22(a)]. A series of mixed-ligand polymers with oba ligand in the presence of neutral N-donor ligands were

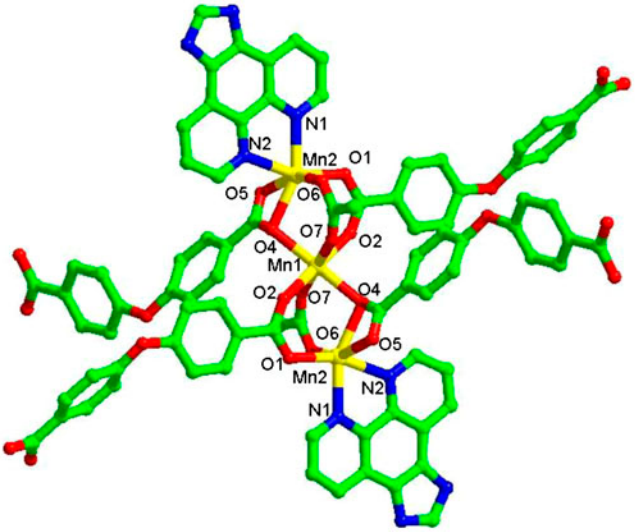

Figure 1. The coordination geometry of the metal centers and the ligand geometry in **1**.

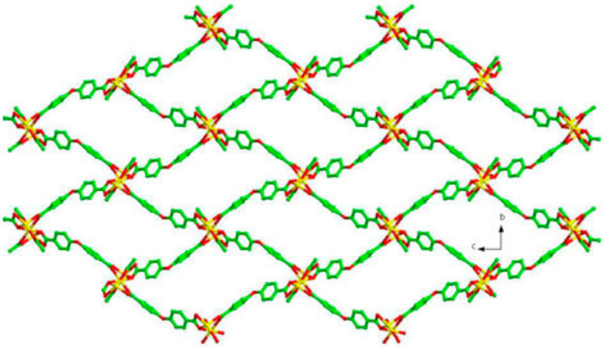

Figure 2. View of a single 2-D layer in the structure of **1**.

prepared [22(a)]; this work indicates that different flexible and angular neutral ligands, coordination geometries of metal centers and weak interactions are crucial factors for formation of the different structures [22(b)]. Although two Cu-oba-bimb coordination polymers were obtained from the same raw materials, the resulting nets are different due to different reaction temperatures and different pH values [22(c)]. LaDuca reported a $[\mathrm{Co_3(oba)_3(bpmp)_2}]_n$ coordination polymer possessing a 3-D self-catenated structure with an unprecedented 8-connected uninodal $4^4 5^{17} 6^7$ topology. The network is formed by the junction of $\{\mathrm{Co_3O_2}\}$ clusters into three different homo-chiral interlocked helical motifs [22(d)]. Three new zinc(II) coordination polymers, $[\mathrm{Zn(imi)_2(\mu_2\text{-}oba)}]_n\cdot n\mathrm{H_2O}$, $[\mathrm{Zn(2,2'\text{-}bipy)(\mu_2\text{-}oba)(H_2O)}]_n\cdot n\mathrm{H_2O}$, and $[\mathrm{Zn_2(4,4'\text{-}bipy)(\mu_2oba)_2(H_2O)_2(DMF)_2}]_n\cdot n\mathrm{DMF}$ (imi = imidazole), have 1-D nano-dimensional pore and square grid structures, respectively [22(e)]. Four cobalt(II) coordination polymers, $[\mathrm{Co_2(oba)_2(1,2\text{-}bix)_2}]_n$, $[\mathrm{Co(oba)(1,3\text{-}bix)}]_n$, $\{[\mathrm{Co_4(oba)_4(1,4\text{-}bix)_4}]\cdot 6\,\mathrm{H_2O}\}_n$, and $\{[\mathrm{Co_6(oba)_6(1,4bix)_6}]\cdot 2\mathrm{H_2oba}\cdot 3\mathrm{DMF}\cdot 11\mathrm{H_2O}\}_n$, 1,*n*-bix = 1,*n*-bis(imidazol-l-yl-methyl)benzene ($n = 2$, 3, 4), show 2-D grid net, 2-D structure with two distinct left- and right-handed helical chains, 2-D doubly interpenetrated motif, and 1-D chains of rings, respectively [22(f)]. A 2-D coordination polymer of $[\mathrm{Co(oba)}]_n$ is negligibly magnetically coupled to each other and the single-ion magnetic behavior of Co(II) in octahedral environment is dominant at low temperature [22(g)]. Comparing those structures, neutral bridging ligands can link similar $\mathrm{M^{II}}$-oba units to form higher dimensional structures than neutral terminal ligands. The resulting work can be modulated by the preference of metal centers.

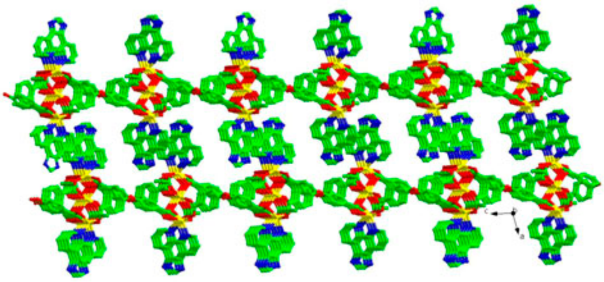

Figure 3. View of the 3-D supramolecular motif in **1**.

IR, TGA, and XRPD

The compound shows a broad band centered around 3468 cm^{-1} attributable to the O–H stretching frequency of water in **1**, as shown in Supplemental data. Asymmetric stretch $v(COO^-)$ appears at 1605 cm^{-1} and the symmetric stretch $v(COO^-)$ at 1480 cm^{-1}. For **1**, the difference between the asymmetric and symmetric stretches, $\Delta v_{as(COO^-)}–v_{s(COO^-)}$, is 125 cm^{-1}, indicating that carboxyl groups are coordinated bidentate, consistent with the observed X-ray crystal structure of **1**.

To study the stability of the polymer, TGA of **1** was performed (Supplemental data), showing two weight loss steps. The first of 10.1% between 20 and 289 °C corresponds to release of one crystallization water and two acetates per formula unit (Calcd 10.8%) and the complex remains undecomposed up to 420 °C. The second decomposition finishes at about 700 °C, which can be attributed to elimination of organic ligands (Calcd 69.8%). Additionally, to confirm the phase purity, the original sample was characterized by XRPD at room temperature. The XRPD pattern of **1** is similar to that of the simulated phase, although minor differences can be seen in the positions, intensities, and widths of some peaks, as shown in Supplemental data.

Magnetism

The $\chi_m T$ *versus* T plots under 1 KOe are shown in figure 4. The $\chi_m T$ value at 300 K is 14.4 cm^3 K M^{-1}, indicating all manganese(II) ions are in the high-spin state. On cooling, $\chi_m T$ decreases to the minimum of 1.49 cm^3 K M^{-1} at 1.8 K, indicating that the dominating interaction is antiferromagnetic [23]. When the structural data of **1** are obtained, three Mn (II) ions are bridged by oba and CH_3COO^-, forming linear Mn^{II}_3 subunits. Assuming that the exchange couplings within the cluster are $J_{12} = J_{23} = J_1$ and $J_{13} = J_{2,}$ where J_{12} and J_{23} are the exchange interactions between central Mn(II) and terminal Mn(II); J_2 is the exchange interaction between terminal Mn(II) ions and intratrinuclear Mn(II)$_3$); zJ' is

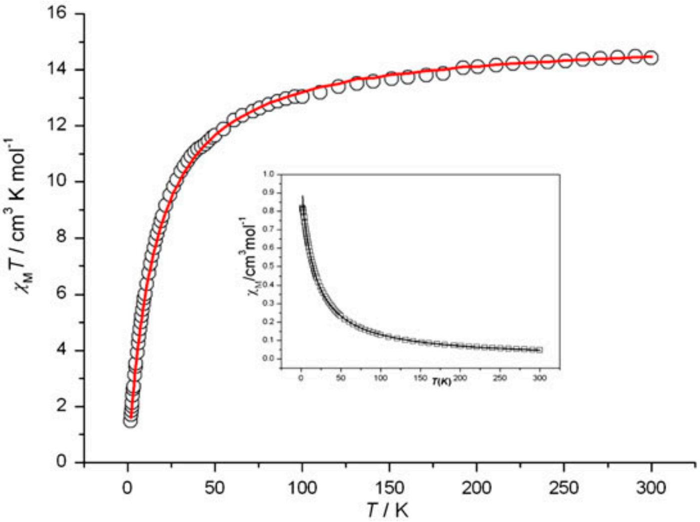

Figure 4. Plots $\chi_M T$ *vs.* T for **1**; red solid lines represent fits to the data. The inset shows a plot $\chi_M T$ *vs.* T in **1** (see http://dx.doi.org/10.1080/00958972.2014.941829 for color version).

referring to the intercluster coupling constants. The variable-temperature magnetic susceptibility data of Mn(II) trimers were fitted according to the equations [24]:

$$E(S,S') = -\frac{J_1}{2}S(S+1) - \frac{J_2 - J_1}{2}S'(S'+1) \tag{1}$$

$$F(J_1,J_2,T) = \frac{1}{3}\frac{\sum_{S'=0}^{5}\sum_{S=|S'-5/2|}^{S'+5/2} S(S+1)(2S+1)\exp\left[-\frac{E(S,S')}{kT}\right]}{\sum_{S'=0}^{5}\sum_{S=|S'-5/2|}^{S'+5/2}(2S+1)\exp\left[-\frac{E(S,S')}{kT}\right]} \tag{2}$$

$$\chi = \frac{Ng^2\beta^2F(J_1,J_2,T)}{kT - zJ'F(J_1,J_2,T)} \tag{3}$$

The best fitting parameters were obtained as $J_1 = -0.47\ \text{cm}^{-1}$, $J_2 = 0\ \text{cm}^{-1}$ (fixed), $g = 2.152$, and $zJ' = -0.99\ \text{cm}^{-1}$ indicating an antiferromagnetic interaction between adjacent Mn(II) ions in a trinuclear cluster. The discrepancy factor defined by $R = \Sigma(\chi_{\text{M,exp}}T - \chi_{\text{M,cal}}T)^2/\Sigma(\chi_{\text{M,exp}}T)^2$ is equal to 2.78×10^{-6}. These values confirm the presence of antiferromagnetic interaction between Mn^{2+} ions within a trinuclear subunit. The intercluster magnetic interaction (zJ') is rather small, indicating that the exchange interactions between two magnetic clusters are very weak, due to the large separations (15.9 Å) between neighboring magnetic subunits. For exchange interaction in these molecules, a superexchange mechanism prevails a main metal–metal interaction, in which the electronic structure of the bridging of the O–C–O moiety determines the magnitude of the antiferromagnetic interaction [24]. The parameter Φ_{bend} of Mn–O–C–O–Mn is very important. The larger Φ_{bend} could generate a larger decrease in $-J$ because of reduced overlap of the d_{x2-y2} orbital with the $2p_x$ carboxylate oxygen orbital in the symmetric HOMO [25]. In the case of **1**, Φ_{bend} is 5.5(3)°, which is slightly smaller than that of $[\text{Mn}_3(\text{L})(\text{DMA})\cdot 2\text{DMA}]$ (H_6L = hexa[4-(carboxyphenyl)oxamethyl]-3-oxapentane acid) [23]. A triangular manganese compound $\{[\text{Mn}_3\text{O}_4(\text{H}_2\text{O})_2(\text{phen})_4](\text{NO}_3)_4\cdot 3\text{H}_2\text{O}\}_n$ with mono-μ-oxo and di-μ-oxo mode shows strong antiferromagnetic coupling between metal ions with the parameters of $g = 1.99$, $J_1 = 50.0\ \text{cm}^{-1}$, and $J_2 = 90.2\ \text{cm}^{-1}$ (where J_1 describes the interaction across the two mono-μ-oxo bridges and J_2 is the exchange coupling across the di-μ-oxo bridge) [26]. Liu *et al.* reported $[\text{Mn}(\text{hfac})_2\text{NIT}(\text{Ph-m-OPh})]$ consists of a 1-D chain with Mn(II) bridged by NIT(Ph-m-OPh). The complex exhibits intramolecular antiferromagnetic interactions between Mn(II) and NIT(Ph-m-OPh) [27]. A trinuclear Mn(II) compound, $[\text{Mn}_3(\text{Hbptc})_2(2,2'\text{-bpy})_3(\text{H}_2\text{O})_8]\cdot 2\text{H}_2\text{O}$ (H_4bptc = iphenyl-2,5,2′,5′-tetracarboxylic acid, 2,2′-bpy = 2,2′-bipyridine), exhibits weak antiferromagnetic interaction. The authors infer that the small Weiss value is indicative of weak antiferromagnetic interactions between neighboring Mn(II) ions, possibly due to a long Mn···Mn distance of 6.801 Å [21(a)]. The magnetic susceptibilities of $\{[\text{Mn}(\mu_{1,3}\text{-N}_3)(\text{phenCl})_2]\cdot(\text{ClO}_4)\}_n$ gave an antiferromagnetic interaction of $J = -5.99\ \text{cm}^{-1}$, which is similar with the magnetic interactions in other Mn(II) complexes with azide as single end–end bridge [28]. A dinuclear complex of manganese(II), $[\text{Mn}(\text{L})(\mu_{1,5}\text{-dca})(\text{CH}_3\text{OH})]_2$, with dicyanamide anion and (E)-3-hydroxy-N′-(pyridin-2-ylmethylene)-2-naphthohydrazide (HL) was synthesized. Magnetic measurements showed an antiferromagnetic interaction between adjacent manganese ions in the dimer [29].

Conclusion

We have presented a rational synthetic strategy for a new Mn(II) compound **1** with mixed ligands. The magnetic behavior of **1** shows the presence of antiferromagnetic interaction between the Mn^{2+} ions within a trinuclear subunit.

Funding

The authors acknowledge financial assistance from Sichuan University of Science and Engineering, the Institute of Functionalized Materials [grant number 2012KY12], [grant number 2014PY01]; the Opening Project of Key Laboratory of Green Catalysis of Sichuan Institutes of High Education [grant number LYJ1207]; the Education Committee of Sichuan Province [grant number 12ZA090], [grant number 13ZB0131], [grant number 14ZB0220]; scientific research plan projects of Shaanxi Education Department [grant number 12JK0608]; and greater contribution from Prof. B. Liu and Hiroshi Sakiyama.

Supplemental data

Supplemental data for this article can be accessed http://dx.doi.org/10.1080/00958972.2014.941829.

References

[1] S. Ma, D. Yuan, X.S. Wang, H.C. Zhou. *Inorg. Chem.*, **48**, 2072 (2009).
[2] B.L. Chen, S.C. Xiang, G.D. Qian. *Acc. Chem. Res.*, **43**, 111 (2010).
[3] D.L. Long, R.J. Hill, A.J. Blake, N.R. Champness, P. Hubberstey, C. Wilson, M. Schröder. *Chem. Eur. J.*, **11**, 1384 (2005).
[4] L. Carlucci, G. Ciani, D.M. Proserpio. *Coord. Chem. Rev.*, **246**, 247 (2003).
[5] S.Q. Ma, J. Eckert, P.M. Forster, J. Yoon, Y.K. Hwang, J.S. Chang, C.D. Collier, J.B. Parise, H.C. Zhou. *J. Am. Chem. Soc.*, **130**, 15896 (2008).
[6] X.M. Chen, G.F. Liu. *Chem. Eur. J.*, **8**, 4811 (2002).
[7] C.Y. Sun, S. Gao, L.P. Jin. *Eur. J. Inorg. Chem.*, **12**, 2411 (2006).
[8] J.Q. Liu, Y.Y. Wang, P. Liu, Z. Dong, Q.Z. Shi, S.R. Batten. *CrystEngComm*, **11**, 207 (2009).
[9] J.J.M. Amoore, C.A. Black, L.R. Hanton, M.D. Spicer. *Cryst. Growth Des.*, **5**, 1255 (2005).
[10] M. Kurmoo. *Chem. Soc. Rev.*, **38**, 1353 (2009).
[11] B.C. Tzeng, T.H. Chiu, B.S. Chen, G.H. Lee. *Chem. Eur. J.*, **14**, 5237 (2008).
[12] (a) Z.B. Zheng, R.T. Wu, J.K. Li, Y.F. Sun, Y.F. Han. *J. Mol. Struct.*, **964**, 109 (2010); (b) M. Du, C.P. Li, C.S. Liu, S.M. Fang. *Coord. Chem. Rev.*, **257**, 1282 (2013); (c) M. Du, X.J. Jiang, X.J. Zhao. *Inorg. Chem.*, **46**, 3984 (2007); (d) A.K. Pramanik, M.S. Jana, T.K. Mondal. *J. Coord. Chem.*, **66**, 4067 (2013).
[13] W.H. Huang, L. Hou, B. Liu, L. Cui, Y.Y. Wang, Q.Z. Shi. *Inorg. Chim. Acta*, **382**, 13 (2012).
[14] G.M. Sheldrick. *SHELXL-97: Program for Structure Determination and Refinement*, University of Göttingen, Göttingen (1997).
[15] A.Y. Robin, K.M. Fromm. *Coord. Chem. Rev.*, **250**, 2127 (2006).
[16] H.J. Chen, Z.W. Mao, S. Gao, X.M. Chen. *Chem. Commun.*, 2320 (2001).
[17] R. Wang, E. Gao, M. Hong, S. Gao, J. Luo, Z. Lin, L. Han, R. Cao. *Inorg. Chem.*, **42**, 5486 (2003).
[18] M.H. Zeng, M.C. Wu, H. Liang, Y.L. Zhou, X.M. Chen, S.W. Ng. *Inorg. Chem.*, **46**, 7241 (2007).
[19] F.Y. Yi, Z.M. Sun. *Cryst. Growth Des.*, **12**, 5693 (2012).
[20] J.P. Zhao, R. Zhao, W.C. Song, Q. Yang, F.C. Liu, X.H. Bu. *Cryst. Growth Des.*, **13**, 437 (2013).
[21] (a) D. Tian, Y. Pang, S. Guo, X. Zhu, H. Zhang. *J. Coord. Chem.*, **64**, 1006 (2011); (b) J. Raymond, R.E. Blankenship. *Coord. Chem. Rev.*, **252**, 377 (2008).
[22] (a) K.S. Diao, L. Li, Y.Q. Ding, F.H. Lei. *Molecules*, **17**, 11103 (2012); (b) Y.Q. Lan, S.L. Li, Y.M. Fu, Y.H. Xu, L. Li, Z.M. Su, Q. Fu. *Dalton Trans.*, 6796 (2008); (c) F. Wang, X.H. Ke, J. Zhao, K.J. Deng, X.K. Leng, Z.F. Tian, L.L. Wen, D.F. Li. *Dalton Trans.*, 11856 (2011); (d) D.P. Martin, R.J. Staples, R.L. LaDuca. *Inorg. Chem.*, **47**, 9754 (2008); (e) X.P. Xiao, S. Aghabeygi, S.S. Wang, H.Y. Wu, C.E. Tong, W.B. Zhang, A. Morsali. *J. Coord. Chem.*, **66**, 1821 (2013); (f) B.F. Huang, H.P. Xiao, H. Huang, X.H. Li, J.G. Wang, A. Morsali. *J. Coord. Chem.*, **66**, 904 (2013); (g) G.H. Wu, Y.X. Han, D.Y. Wu, W. Huang, X.H. Zhou. *J. Coord. Chem.*, **65**, 681 (2012).

[23] (a) K.F. Hsu, S.L. Wang. *Inorg. Chem.*, **39**, 1773 (2000); (b) A.D. Burrows, C.G. Frost, M.F. Mahon, M. Winsper, C. Richardson, J.P. Attfield, J.A. Rodgers. *Dalton Trans.*, 6788 (2008); (c) C.P. Landee, M.M. Turnbull. *J. Coord. Chem.*, **67**, 375 (2014).

[24] O. Kahn. *Molecular Magnetism*, p. 211, VCH Publishers, New York (1993).

[25] (a) J.L. Manson, E. Ressouche, J.S. Miller. *Inorg. Chem.*, **39**, 1135 (2000); (b) Y.M. Song, X.F. Feng, F. Luo. *J. Coord. Chem.*, **65**, 2705 (2012).

[26] B. Biswas, A. Pal, P. Mitra, F. Tuna, M. Mukherjee, R. Ghosh. *J. Coord. Chem.*, **65**, 4067 (2012).

[27] X.Y. Qin, G. Xiong, D.Z. Liao, Y. Ma, P. Gao, X.L. Sun, P. Liu. *J. Coord. Chem.*, **65**, 2683 (2012).

[28] (a) Y.Y. Wang, Q.H. Liu, W.W.H. Du, J.M. Shi, Y.Q. Zhang. *J. Coord. Chem.*, **66**, 254 (2013); (b) A.K. Sra, J.-P. Sutter, P. Guionneau, D. Chasseau, J.V. Yakhmi, O. Kahn. *Inorg. Chim. Acta*, **300**, 778 (2000); (c) P.-Y. Bu, L.-Z. Zhang, L.-C. Li, Y. Dai, P. Cheng, S.-P. Yan, D.-Z. Liao. *J. Coord. Chem.*, **55**, 1263 (2002); (d) S. Miller, M. Drillon. *Magnetism Molecules to Materials: Models and Experiments*, Wiley-VCH, Weinheim (2002).

[29] R. Bikas, H. Hosseini-Monfared, L. Sieroń, A. Gutiérrez. *J. Coord. Chem.*, **66**, 4023 (2013).